

First-principles calculations of second-order nonlinear optical coefficients in the static limit and Pockels coefficients in III-N and II-IV-N₂ compounds

Sai Lyu and Walter R. L. Lambrecht

Department of Physics, Case Western Reserve University, 10900 Euclid Avenue, Cleveland, Ohio 44106-7079, USA



(Received 17 October 2018; published 5 December 2018)

The second-order nonlinear optical coefficients in the static limit are evaluated using density functional perturbation theory from the electronic response to a static electric field for the group-III nitrides and several II-IV-N₂ ternary nitrides. They are compared with literature results using the sum over states approach including local field effects. The effects of the scissor correction are evaluated. Good agreement is obtained for GaN, AlN, and w-BN. For InN, the small or even negative gap in the LDA at Γ causes an extreme sensitivity to the \mathbf{k} point summation and pseudopotentials. Similar problems occur for other very small gap II-IV-N₂ semiconductors. The nonlinear optics coefficients are showing a general trend of increasing values with smaller gaps but no clear scaling relation with the direct gaps is obtained. In addition, unexpected changes in sign are found for the Si-based compounds, similar to the case of AlN, compared to the expected signs of d_{33} in GaN. The Pockels coefficient, which includes in addition to the electronic response the phonon and piezoelectric response, is also evaluated. They show that the phonon and electronic contributions to the response in these materials are comparable in magnitude but in many cases of opposite sign.

DOI: [10.1103/PhysRevMaterials.2.124602](https://doi.org/10.1103/PhysRevMaterials.2.124602)

I. INTRODUCTION

Nonlinear optical properties are of interest both from an applied and fundamental perspective. They can be used for frequency conversion via sum and difference frequency generation, including second harmonic generation. The calculation of frequency-dependent second-order nonlinear optical coefficients in solids is rather complex because of difficulties in obtaining divergence free expressions in perturbation theory within the usually applied momentum gauge [1]. This problem was solved within the independent particle approach in a series of papers by Sipe and collaborators [2–4]. However, these formulations still do not include local field effects or excitonic effects. A formulation for the frequency dependent second-harmonic generation including local field effects was obtained by Levine [5,6] but in practice applied only for the region below the gap. In this treatment, only first-order local field effects were included while in a subsequent paper, second-order local field effects were found not to be negligible but expressible in terms of the first-order ones in the static limit [7]. We will refer this as the “sum over states” approach. Methods for including excitonic effects were also recently developed [8,9] and specialized to 2D materials but were thus far restricted to simplified models of the band structure with a few bands and $\mathbf{k} \cdot \mathbf{p}$ type models.

On the other hand, in applications, one is usually interested mostly in the region below the gap and in the static limit, for which an alternative simpler formulation of the second harmonic effects can be obtained by calculating the response to a static electric field by means of a Berry phase calculation of the polarization [10,11]. Because of the $2n + 1$ theorem in density functional perturbation theory (DFPT), one can calculate up to third derivatives of the total energy from the first-order corrected wave functions. So, a first-order corrected

wave function in response to a static electric field allows one to calculate the third-order derivatives of the total energy versus a static electric field, and these provide precisely the static limit of the second-order nonlinear optics response functions. This approach was first proposed by Dal Corso *et al.* [12,13].

Our first goal here is to compare this approach for the group-III nitride semiconductors with the alternative methods and with experiment. We then also apply the same approach to various II-IV-N₂ semiconductors. The latter have recently gained increasing interest [14–33]. We note that for other III-V semiconductors than nitrides, the corresponding chalcopyrite II-IV-V₂ semiconductors, such as ZnGeP₂ and CdGeAs₂ have found applications in nonlinear optics. This is not only because they have relatively high second-order susceptibilities $\chi^{(2)}$, but also because the lower (tetragonal) symmetry allows for birefringence and phase matching and hence more efficient frequency conversion than in III-V materials. While the nitrides with higher band gaps are expected to have lower $\chi^{(2)}$, there still is a fundamental interest in comparing the nonlinear optics response of the corresponding III-N with the II-IV-N₂ families.

The above considered static nonlinear optical response concerns only electronic response and thus applies only to the frequency range well below the band gap but still high with respect to phonon frequencies. In the true static limit, additional response from the phonons comes into play. This leads to the linear electro-optic (EO) or Pockels effect [34]. The EO tensor $r_{ij\gamma}$ describes the change in the inverse dielectric constant ε in response to a static electric field $\vec{\mathcal{E}}$:

$$\Delta(\varepsilon^{-1})_{ij} = r_{ij\gamma} \mathcal{E}_\gamma, \quad (1)$$

where summation convention over repeated indices is used. It includes an electronic, ionic, and piezoelectric contribution. Here, i and j refer to Cartesian components of the optical frequency fields, i.e., above the phonon range, where γ refers to a static field. We may view this as a sum frequency $\omega + 0 = \omega$ NLO effect. The purely electronic part of the linear EO effect can thus indeed be written in terms of the $\chi_{ij\gamma}^{(2)}$ as

$$r_{ij\gamma}^{el} = -8\pi(\epsilon^{-1})_{il}\chi_{lm\gamma}^{(2)}(\epsilon^{-1})_{mn}, \quad (2)$$

or assuming the Cartesian axes coincide with the crystal principal axes, so that $\epsilon_{ij} = n_i^2\delta_{ij}$ is diagonal and corresponds to the index of refraction squared (at optic frequencies),

$$r_{ij\gamma}^{el} = -\frac{8\pi}{n_i^2 n_j^2} \chi_{ij\gamma}^{(2)}. \quad (3)$$

The phonon contribution [34] stems from the fact that the linear susceptibility $\chi_{ij}^{(1)}$ (or equivalently ϵ_{ij}) changes when the atoms are displaced and involves $\partial\chi_{ij}^{(1)}/\partial\tau_{n\alpha}$, where $\tau_{n\alpha}$ is the displacement of atom n in the unit cell in direction α . It thus involves the Born effective charges and the m th mode Raman tensor α^m ,

$$r_{ij\gamma}^{ion} = -\frac{4\pi}{\sqrt{\Omega_0 n_i^2 n_j^2}} \alpha_{ij}^m P_\gamma^m \quad (4)$$

with the mode polarity

$$P_\gamma^m = \sum_n Z_{n,\gamma\beta}^* u_m(n\beta) \quad (5)$$

with $Z_{n,\gamma\beta}^*$ the Born effective charge and $u_m(n\beta)$ the mode eigenvector in terms.

Finally, at even lower frequencies, a piezoelectric contribution comes in because the electric field induces a change in lattice constants or strain via the piezoelectric effect, which in turn induces an optoelastic effect. This contribution is written as [34]

$$r_{ij\gamma}^{piezo} = p_{ij\mu\nu} d_{\gamma\mu\nu} \quad (6)$$

in terms of the optoelastic tensor $p_{ij\mu\nu}$, which describes the linear change in $\chi_{ij}^{(1)}$ in response to a strain $\eta_{\mu\nu}$ and the piezoelectric tensor $d_{\gamma\mu\nu}$, which gives the strain $\eta_{\mu\nu} = d_{\gamma\mu\nu} \mathcal{E}_\gamma$ induced by the electric field. The calculation of derivatives of total energy versus atomic displacement, strain [35,36], and electric fields have all been worked out in DFPT. When the piezoelectric contribution is not included, one calls the Pockels effect clamped, otherwise unclamped. The clamped value corresponds to frequencies sufficiently high that the lattice constant or unit cell shape relaxation via the piezoelectric effect can be neglected, typically above 100 MHz. In some materials, such as typical ferroelectrics, the ionic contribution can be the dominant one and allows in principle to tune optical properties via electric effects.

II. COMPUTATIONAL METHOD

The basic framework for our calculations is density functional (DFT) [37,38] and density functional perturbation theory (DFPT) [10,11]. The DFPT approach provides a method to calculate the response of an insulating system to adiabatic (with respect to electronic time scales) perturbations, such as

a static or slowly varying electric field, atomic displacements, and strain. DFPT using first-order corrected wave functions allows one to calculate up to third-order derivatives of the total energy [34]. As mentioned already in Introduction, the third-order derivative of the total energy as a function of a static electric field gives us the second-order susceptibility and when adding the appropriate phonon response parts the Pockels coefficient.

All the calculations are done with the ABINIT package [39] in the local-density approximation (LDA). LDA is used rather than the generalized gradient approximation (GGA) here for easier comparison to previous work. Various pseudopotentials were tested, among them the norm-conserving Fritz-Haber pseudopotential [40], and the Hartwigsen-Goedecker-Hutter [41] pseudopotentials. An 80-Ha plane-wave energy cutoff and a $4 \times 4 \times 4$ Monkhorst-Pack \mathbf{k} -point mesh are used to perform the calculations for II-IV-N₂ compounds, except for MgSiN₂ where a $6 \times 6 \times 6$ mesh was used. For the III-N compounds, the plane-wave energy cutoff and \mathbf{k} -point mesh were set to be 80 Hartree and $8 \times 8 \times 4$, except for InN where a $12 \times 12 \times 8$ mesh was used.

As we will see, an issue to be studied is how the underestimate of the gap by the local density approximation or semilocal generalized gradient approximation (GGA) affects the results. Although the interband transitions in this approach do not directly enter the calculations, one may still include a so-called scissor's operator correction to the gap [11]. This in fact enters when solving the Sternheimer equation for the first-order corrected wave functions as was discussed in Appendix A of Ref. [11]. Additionally, all the calculations within DFPT assume that there is a gap. In some cases, such as InN, the gap in LDA vanishes. We avoid the closing of the gap by using a shifted mesh, which does not include the Γ point in the Brillouin zone integrations and which is coarse enough to avoid points where the gap closes, while still being sufficiently accurate to sample the Brillouin zone. Nonetheless, the region close to Γ where the gap and hence energy denominators in the perturbation theory approach would be very small may dominate the result and give unphysical results. To further investigate the problem, we also used different pseudopotentials, for example not including the lower In $4d$ states as bands, which tends to lower the VBM and allows us to open a gap. Nonetheless we will see that for these cases, the results are very sensitive to the mesh and the pseudopotential, and extracting a meaningful result is not evident.

III. RESULTS

A. Nonlinear optical tensor

We start by comparing the static second harmonic response obtained from the $(2n + 1)$ approach in wurtzite III-N semiconductors with the "sum over states" approach including local field corrections [7] and experiment in Table I. Note that we use the Voigt notation for third-rank tensors. In the expression for the polarization $P_i = \chi_{ijk}^{(2)} \mathcal{E}_j \mathcal{E}_k$, the last two indices are contracted to $\chi_{im}^{(2)}$, where $m = 1, 2, 3, 4, 5, 6$ for $\{jk\} = xx, yy, zz, yz = zy, zx = xz, xy = yx$. Furthermore, we use the usual notation $d_{im} = \frac{1}{2} \chi_{im}^{(2)}$. In wurtzite crystals by symmetry, the only nonzero coefficients are d_{31} and d_{33} . Because

TABLE I. Second-order nonlinear optical tensor coefficients d_{im} in pm/V, optical dielectric constants ϵ^∞ (averaged over directions) and band gap for wurtzite III-N semiconductors at experimental lattice constants. Results obtained with various pseudopotentials and obtained with the sum over states approach including local fields [7] are included as well as the effects of the scissor correction, and experimental values where available. For GaN, AlN, and InN, the scissor correction is taken as the difference between the experimental gap and the gap with a particular pseudopotential, for BN, we use the fixed value 2.5 eV used by Chen *et al.* [7]. The band gaps E_g are the direct gaps at Γ , which are indeed the minimum gaps for AlN, GaN, and InN. For w-BN, the minimum gap is at K , 3.2 eV below that of Γ .

Psp.	property	BN		AlN		GaN		InN	
		(2n + 1) approach							
		LDA	scissor	LDA	scissor	LDA	scissor	LDA	scissor
FHI ^a	d_{31}	-1.38	-0.89	-0.13	-0.07	-2.80	-1.97	8469	765
	d_{33}	2.70	1.77	-3.54	-2.27	4.78	3.37	-506	-139
	d_{31}/d_{33}	-0.51	-0.50	0.04	0.03	-0.59	-0.58	-16.8	-5.5
	E_g	8.26	10.76	4.26	6.1	2.17	3.51	0.30 ^b	0.7
	ϵ^∞	4.58	4.00	4.48	3.87	5.57	4.83	15.21	8.91
KA	d_{31}	-1.37	-0.89	-0.19	-0.09	-3.71	-2.90	-10.92	-13.5
	d_{33}	2.69	1.76	-3.60	-2.18	5.83	4.46	25.45	31.4
	d_{31}/d_{33}	-0.51	-0.51	0.05	0.04	-0.64	-0.65	-0.43	-0.43
	E_g	8.29	10.79	4.23	6.1	2.73	3.51	0.89	0.7
	ϵ^∞	4.54	3.97	4.50	3.88	5.34	4.93	6.51	7.26
HGH	d_{31}	-1.41	-0.90	-0.11	-0.05	-3.12	-2.27	90	34.6
	d_{33}	2.80	1.80	-3.60	-2.21	5.23	3.80	-20	-7.5
	d_{31}/d_{33}	-0.50	-0.50	0.03	-0.02	-0.60	-0.60	-4.5	-4.6
	E_g	8.23	10.73	4.23	6.1	2.39	3.51	0.34	0.7
	ϵ^∞	4.61	4.03	4.50	3.90	5.47	4.87	8.35	7.32
FHI (semicore)	d_{31}					-2.19	-1.82	10200	607
	d_{33}					3.58	3.15	-198	-58
	d_{31}/d_{33}					-0.61	-0.58	52	10.5
	E_g (direct)					1.76	3.51	0.22 ^b	0.7
	ϵ^∞					6.21	5.10	22.3	10.5
HGH(semicore)	d_{31}					-2.46	-2.04	9302	665
	d_{33}					3.99	3.18	-302	-85
	d_{31}/d_{33}					-0.62	-0.59	-31	-7.8
	E_g (direct)					1.83	3.51	0.25 ^b	0.7
	ϵ^∞					6.13	5.09	18.83	9.84
		sum over states ^c							
		LDA	scissor	LDA	scissor	LDA	scissor		
	d_{31}	-1.4	-0.9	-0.1	-0.1	-3.2	-2.1		
	d_{33}	2.7	1.7	-4.2	-2.3	5.4	3.5		
	d_{31}/d_{33}	-0.52	-0.53	0.02	0.04	-0.59	-0.60		
		Expt.							
	d_{31}			$ d \leq 0.26^d$		2.66 ^e			
	d_{33}			-6.3 ± 3.5		-5.35			
	d_{31}/d_{33}			≤ 0.04		-0.50			
	E_g			6.1 ^f		3.51 ^g		0.7 ^h	
	ϵ^∞			4.22 ⁱ		5.35 \pm 0.2 ^j (ordinary)		8.4 ^k , 5.8 ^l	

^aThe pseudopotentials choices are as follows: FHI Fritz-Haber Institute Troullier-Martins type pseudopotentials [40], KA, A. Khein, D. C. Allan pseudopotentials from ABINIT web site based on Troullier Martins approach, HGH Hartwigsen Goedecker-Hutter [41], semicore means the 3d of Ga and 4d of In are treated as valence states.

^bThis is the smallest gap or the k-mesh used, while the gap at Γ is negative.

^cFrom Chen *et al.* [7].

^dFrom Fujii *et al.* [42].

^eFrom Miragliotta *et al.* [43].

^fFrom Li *et al.* [44].

^gFrom Vurga *et al.* [45].

^hFrom Yu *et al.* [46].

ⁱFrom Moore *et al.* [47].

^jFrom Barker *et al.* [48].

^kFrom Tansley *et al.* [49].

^lFrom Inushima *et al.* [50].

of the equivalence of wurtzite basal plane (0001) with the cubic (111) plane and assuming a quasicubic model, one expects $d_{33} = -2d_{31}$ in wurtzite and $d_{33}^w = \frac{2}{\sqrt{3}}d_{13}^z$, where the w and z superscripts stand for wurtzite and zincblende.

We have tested the sensitivity of the results to the choice of pseudopotentials. All these pseudopotentials were taken from the ABINIT website [39]. The FHI pseudopotentials are the Fritz-Haber Institute norm-conserving pseudopotentials [40]. As the KA potentials, they are obtained within the Troullier-Martins scheme. The origin of the KA pseudopotentials is not entirely clear from the ABINIT website, but they are mentioned to be developed mostly by A. Khein and D. C. Allan without a clear citation. The HGH are Hartwigsen-Goedecker-Hutter pseudopotentials [41]. Some of these come in two versions, treating the semicore d states ($3d$ for GaN and $4d$ for InN) as bands or included in the core. All these calculations are carried out at the experimental lattice constants to avoid any possible errors inherent to the DFT on the lattice constants.

For GaN, we can see that the HGH pseudopotential without semicore d states best reproduces the results of Chen *et al.* [7] but the other ones give d_{im} results that differ by a few 0.1. The ratio of d_{31}/d_{33} is 0.60 ± 0.02 and is well reproduced independent of pseudopotential. The experimental d_{31} is in best agreement with the HGH pseudopotential including the $3d$ semicore states as bands but the d_{33} is then somewhat underestimated. Note that the sign of all the coefficients in the experiment is opposite to the calculated one, but the sign is difficult to determine experimentally and depends on the choice of the orientation of the axes in these polar materials. Our calculated sign corresponds to the positive c direction being oriented from Ga to N along the bonds. To estimate the effect of using experimental instead of calculated lattice parameters we evaluated GaN with the FHI pseudopotentials (including semicore), which is 0.5 % lower in volume than experiment and found $d_{31} = -2.15$ pm/V and $d_{33} = 3.37$ pm/V, so about 6% smaller, which is consistent with a larger gap.

For AlN, surprisingly, the d_{31}/d_{33} ratio is far from the expected quasicubic result but this is well reproduced both by the Chen *et al.* [7] and our present results. Essentially, d_{31} becomes almost negligible and of the same sign as d_{33} . This strong deviation from the quasicubic rule is also obtained using a sum-over-states method without local field effects [51,52]. The different pseudopotentials agree closely with each other in this case but the value closest to Chen *et al.* [7] is obtained again with the HGH pseudopotential. Both ours and Chen *et al.* underestimate the experimental value of $d_{33} = -6.3$ but note the large experimental uncertainty in this value. The calculated value falls within the uncertainty range of the experiment.

For wurtzite BN, the agreement between the different pseudopotentials is excellent and the results also closely agree with those of Chen *et al.* [7]. Because the gap of wurtzite BN is actually indirect, and not well known, we use the same scissor correction as used by Chen *et al.* [7], which is 2.5 eV. The gap quoted in the Table I is the direct gap at Γ . The gap of cubic (zincblende) BN is 6.4 eV experimentally and about 4.2 eV in LDA, but corresponds to the indirect Γ -X gap. In w-BN, the minimum gap is between the valence band maximum (VBM) at Γ and the conduction band minimum (CBM) at K and is

again significantly lower (by about 3.2 eV) than the direct gap at Γ .

We next note that when applying a scissor correction to open the gap, the d_{im} values as well as the ϵ^∞ are reduced as expected. It is not clear, however, that this improves the agreement with experiment. We can see that the scissor correction reduces the d_{im} in a similar manner in the $(2n + 1)$ approach used here as in the sum-over-states method used by Chen *et al.* [7].

For InN, there are no experimental values, and a previous calculation work by Gavrilenko *et al.* [53] gives $d_{33} = 6.17$ pm/V and $d_{31} = 5.62$ pm/V. However, in Ref. [53], the local-field effects were neglected and an overestimated band gap (1.9 eV) was used in the calculation, which would underestimate the resultant second-order optical tensor. Calculating the $\chi^{(2)}$ of InN is problematic because the LDA gives a negative gap and the Berry-phase approach requires a gap to exist. That is, the Γ_{1c} state (which is the CBM at Γ in AlN and GaN) lies below the Γ_{5v} state, which normally forms the VBM. We see that even when we avoid the actual closing of the gap by using a finite ($12 \times 12 \times 8$) and shifted \mathbf{k} mesh, the values of the d_{im} become extremely high and furthermore the order and sign of d_{33} and d_{31} is inverted from that of the other compounds. Even after adding a scissor correction, the values are extremely high. On the other hand, when we use the KA pseudopotential at the experimental lattice constant, a gap at Γ of 0.89 eV opens up, even larger than the experimental value of 0.7 eV. This band structure apparently yields more reasonable looking d_{im} , in particular, d_{31} is negative and d_{33} is positive and about twice as large in absolute value, which is then similar in InN and GaN. The ratio $d_{31}/d_{33} = -0.43$ seems reasonable. After adding a (negative) scissor correction to reduce the gap to 0.7 eV, the values change only slightly and as expected increase slightly. In contrast, using the HGH pseudopotentials, which still have a very small gap at Γ of 0.34 eV, the values are an order of magnitude larger and with an unexpected sign reversal of d_{im} from GaN and an unreasonable $|d_{33}| < |d_{31}|$. Finally, when treating the In $4d$ states as bands, the gap is further reduced and unreasonable values of d_{im} are obtained. Thus, among the various pseudopotentials tested, only the KA choice with or without scissor correction seems to give reasonable results. Although there is still significant uncertainty, the best estimate from the present results would be the scissor corrected ones for the KA pseudopotentials, $d_{33} \approx 30 \pm 5$ and $d_{31} \approx -13 \pm 2$.

To further test this, we plot the d_{33} value as a function of $1/E_g$, with E_g the direct gap at Γ , along the series, BN, AlN, GaN, and InN in Fig. 1. Although the scaling does not correspond to E_g^{-3} as expected on the basis of perturbation theory, these values of InN seem to follow a trend with the other compounds within the III-N family. We have plotted $d_{33}/2$ and $-d_{31}$, which in the quasicubic model would be equal. We can see that AlN is clearly an outlier in the series but the trend from BN to GaN extrapolates reasonably linearly with the inverse gap toward InN and the scissor corrected values also follow the expected trend. Note that the values for InN are about twice those obtained by Gavrilenko *et al.* [53], which makes sense from the point of view that their gap is 1.9 eV.

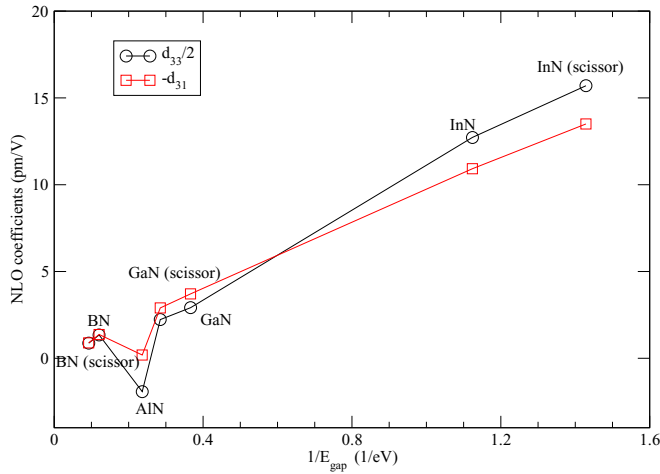


FIG. 1. Second-order NLO coefficients as function of $1/E_g$ for III-N compounds using the KA pseudopotentials.

Next, having established that the approach gives results in good agreement with the sum over states approach for III-N materials, and reasonable agreement with experiment for GaN and AlN, we move on to the II-IV-N₂ semiconductors. For these materials, because of the orthorhombic symmetry, there are three distinct nonzero coefficients, $d_{15} = d_{31}$, $d_{24} = d_{32}$, and d_{33} . The equalities apply only in the static limit and are due to Kleinman permutation symmetry. The difference between d_{32} and d_{31} is expected to be small if the crystal stays close to the hexagonal underlying wurtzite lattice and from the relation with wurtzite, we would expect $d_{33} \approx -2d_{31} \approx -2d_{32}$. The results for these coefficients along with the LDA band gaps and all calculated with the HGH pseudopotential [41], chosen because they appeared to give the best results for GaN, AlN, and BN, are given in Table II.

The band gaps in LDA are close to those reported earlier obtained using the all-electron linearized muffin-tin orbital method [21]. For easier comparison, we give here just the gaps at Γ but we note that in the Si-containing compounds the gap is actually indirect and even in CdGeN₂ the gap is very slightly indirect. The trends are not obvious at all. For ZnGeN₂, which is close to GaN, we see that indeed a similar value of d_{33} is found as for GaN and the $d_{31} \approx d_{32} = -d_{33}/2$.

In fact, we show in Table II the ratio $d_{33}/(d_{31} + d_{32})$, which is expected to be close to -1 . We can see that for the Mg compounds this ratio is significantly smaller and for both MgSiN₂ and ZnSiN₂ the sign of this ratio is reversed as is also the case in AlN. The deviations from these expected ratios indicate the significant deviation of the structure from the ideal wurtzite structure. For both ZnSnN₂ and CdSnN₂, the sign of d_{33} is reversed compared to the corresponding Ge based compounds. We can see a general trend of increasing absolute values of the d_{33} with lower band gap but no clear scaling is apparent. As an example, we show the d_{33} values obtained within the HGH pseudopotential for the three families as a function of $1/E_g$ in Fig. 2. It should be kept in mind that NLO properties involve a rather complex interplay between different interband transitions and are obtained by integrating over the whole Brillouin zone, and hence a simple scaling with band gaps should actually not be expected. We note that

TABLE II. Second-order nonlinear optical tensor coefficients d_{im} in pm/V and LDA direct band gaps at Γ (in eV) calculated for three families of II-IV-N₂ semiconductors.

	MgSiN ₂	MgGeN ₂	MgSnN ₂
	HGH pseudopotentials		
$d_{15} = d_{31}$	-1.57	-1.73	-1.25
$d_{24} = d_{32}$	-0.32	-1.70	-2.98
d_{33}	-0.76	1.35	1.14
$d_{33}/(d_{31} + d_{32})$	0.40	-0.39	-0.27
E_g	4.60	3.24	1.67
	ZnSiN ₂	ZnGeN ₂	ZnSnN ₂
	HGH pseudopotentials		
$d_{15} = d_{31}$	-2.44	-2.55	3.71
$d_{24} = d_{32}$	-1.05	-2.43	1.00
d_{33}	2.80	4.16	-6.00
$d_{33}/(d_{31} + d_{32})$	-0.80	-0.84	-1.27
E_g	3.90	2.29	0.67
	CdSiN ₂	CdGeN ₂	CdSnN ₂
	HGH pseudopotentials		
$d_{15} = d_{31}$	-4.31	-3.77	9.41
$d_{24} = d_{32}$	0.51	0.29	10.44
d_{33}	6.51	4.40	-18.97
$d_{33}/(d_{31} + d_{32})$	-1.71	-1.27	-0.96
E_g	2.32	1.46	0.21
	FHI pseudopotentials		
$d_{15} = d_{31}$	-5.09	-3.94	12.32
$d_{24} = d_{32}$	0.44	1.05	17.39
d_{33}	7.99	4.30	-30.28
$d_{33}/(d_{31} + d_{32})$	-1.72	-1.49	-1.02
E_g	2.17	1.39	0.25
	FHI pseudopotentials + scissor		
$d_{15} = d_{31}$	-3.00	-2.90	5.06
$d_{24} = d_{32}$	-0.20	0.07	7.72
d_{33}	4.89	3.76	-14.77
$d_{33}/(d_{31} + d_{32})$	-1.53	-1.33	-1.16
E_g^a	3.82	2.71	0.84

^aQuasiparticle self-consistent gaps in the 0.8Σ approximation at the LDA lattice constants from Lyu *et al.* [21].

our values for the Zn compounds differ substantially from the values in Paudel *et al.* [16]. The latter were calculated with the FHI pseudopotential, but we found that the real reason for the discrepancy is that only a $2 \times 2 \times 2$ \mathbf{k} -point mesh was used in that work. We have tested that with the here used $4 \times 4 \times 4$ mesh, results closer to the HGH pseudopotential were obtained.

For CdSnN₂, which is very close in band gap to InN, we again obtain values of the order of about 10 for d_{31} and d_{32} and about 20 for d_{33} . With the FHI pseudopotentials, we obtained even larger values but which are then again reduced if we add the scissor correction. Clearly, there is still a significant uncertainty on these values associated with the choice of pseudopotentials for small gap materials.

From a practical point of view, we should note that even for the small gap compounds here, InN, CdSnN₂, and ZnSnN₂, the values are relatively low compared to those of other

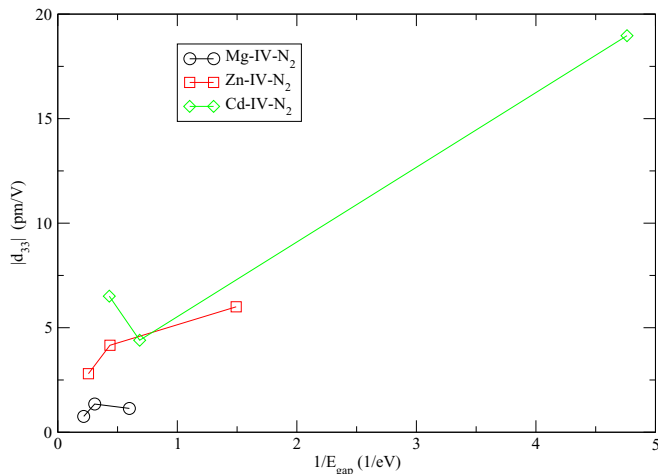


FIG. 2. NLO coefficient d_{33} in pm/V as function of inverse gap in the II-IV- N_2 compounds.

II-IV- V_2 compounds, such as $ZnGeP_2$ and $CdGeAs_2$, where values of order 100 or larger are not uncommon [54].

B. Electro-optic tensor

We start again by establishing the accuracy of the methodology for III-N materials where comparison to experiment is possible. The clamped linear electro-optical coefficients for the III-N compounds are given in Table III. The allowed coefficients are r_{51} , r_{13} , and r_{33} , where the first index is a contracted Voigt index 1-6 and refers to the optic frequency electric fields, and the last index refers to the static electric field. In the Pockels coefficient, unlike the purely electronic nonlinear susceptibility, $r_{51} \neq r_{13}$ because we can no longer permute all indices, since the third one has a different meaning of a truly static electric field. In this part of the work, we performed all the calculations at the experimental lattice constants. We have seen in the previous section that

TABLE III. Clamped linear electro-optical coefficients (pm/V) for BN, AlN, and GaN. The experimental values are given in absolute values.

		r_{51}	r_{13}	r_{33}
BN	FHI	0.005	-0.08	0.38
	HGH	0.005	-0.07	0.38
AlN	FHI	-0.57	-0.86	2.49
	FHI-revised	-0.64	-0.97	2.81
	HGH	-0.56	-0.85	2.45
	HGH-revised	-0.64	-0.97	2.79
	Expt. [55]		0.98	
	Expt. [56]		0.67	-0.59
GaN	FHI	-0.29	-0.63	1.09
	FHI-revised	-0.31	-0.68	1.18
	HGH	-0.30	-0.65	1.20
	HGH-revised	-0.31	-0.68	1.26
	Expt. [57]	0.38	0.72	1.31
	Expt. [58]		0.57	1.91
	Expt. [59]		1.00	1.60

TABLE IV. Decomposition of clamped linear electro-optical coefficients in BN, AlN, and GaN using HGH at experimental lattice constants.

		r_{51}	r_{13}	r_{33}
BN	total	0.005	-0.07	0.38
	electronic	0.26	0.27	-0.50
	phonon	-0.26	-0.34	0.88
AlN	total	-0.56	-0.85	2.45
	electronic	0.02	0.02	0.67
	phonon	-0.58	-0.87	1.78
GaN	total	-0.30	-0.65	1.20
	electronic	0.41	0.42	-0.68
	phonon	-0.71	-1.07	1.88

the NLO coefficient is not clearly improved in comparison to experiment by adding the scissor correction, nor are the ϵ^∞ . The LDA values seem a bit overestimated, while the scissor corrected ones seem underestimated. In fact, it has been suggested [34] to improve the estimated electro-optical coefficients by adjusting the dielectric constants or indices of refraction appearing in the equations to experimental values. This is what we also do here in the results listed as “revised.” The averaged LDA dielectric constant for GaN with the FHI pseudopotential and at the experimental lattice constant is 5.57 and the experimental high-frequency dielectric constant $\epsilon^\infty = 5.35$, and we here ignore the directional dependence because it is small. We make similar adjustments for HGH results. We can see that our revised results and the HGH results are in good agreement with the experimental value of Ref. [57].

For AlN, we also find the revised results (for both pseudopotentials) to give comparable results. We should also keep in mind that the experimental values show in fact a frequency dependence not yet addressed in the present paper. This arises among other from the dispersion (frequency dependence) of the indices of refraction. The calculated LDA dielectric constants for AlN are 4.48 (at FHI) and 4.50 (at HGH). To obtain the revised values, we use the directionally averaged high-frequency dielectric constants $\epsilon^\infty = 4.22$. The revised results are in good agreement with the more recent Ref. [55], but not with Ref. [56]. Since $|d_{33}| \gg |d_{31}|$ for AlN, one generally expects that r_{33} , due to the electronic contribution, should be notably larger than r_{31} and this is found to be the case even after adding the phonon contributions.

Separately, in Table IV, we show the decomposition of the clamped EO tensor into its purely electronic and phonon parts. This shows that the electronic part has ratios of r_{13}/r_{33} similar to the corresponding second harmonic generation coefficients. However, the phonon part has values of comparable size and opposite sign for r_{13} to the electronic part. As a result, the r_{13} and r_{51} become negligible for BN, and for AlN they become dominated by the phonon part because the electronic part is anomalously small. For AlN, the r_{33} phonon contribution has the same sign as the electronic one, so they enhance each other, while for GaN and BN, they have opposite sign. Again, AlN behaves different from the other materials in this respect. For GaN, we can also compare our results with

TABLE V. Clamped linear electro-optical coefficients (pm/V) for Mg-IV-N₂, Zn-IV-N₂, and Cd-IV-N₂ compounds.

		r_{51}	r_{42}	r_{13}	r_{23}	r_{33}
MgSiN ₂	total	-0.01	-0.36	-0.40	-0.53	1.10
	electronic	0.33	0.07	0.34	0.07	0.16
	phonon	-0.34	-0.43	-0.74	-0.60	0.94
MgGeN ₂	total	-0.07	-0.15	-0.25	-0.19	0.88
	electronic	0.31	0.30	0.32	0.29	-0.23
	phonon	-0.38	-0.45	-0.57	-0.48	1.11
MgSnN ₂	total	-0.40	-0.19	-0.78	-0.48	1.37
	electronic	0.17	0.39	0.18	0.40	-0.15
	phonon	-0.57	-0.58	-0.96	-0.88	1.52
ZnSiN ₂	total	0.24	0.01	-0.07	-0.23	-0.05
	electronic	0.37	0.16	0.37	0.17	-0.41
	phonon	-0.13	-0.15	-0.44	-0.40	0.36
ZnGeN ₂	total	0.16	0.19	-0.08	-0.07	-0.04
	electronic	0.32	0.31	0.33	0.31	-0.51
	phonon	-0.16	-0.12	-0.41	-0.38	0.47
ZnSnN ₂	total	-0.68	-0.37	-1.04	-0.80	1.48
	electronic	-0.32	-0.09	-0.33	-0.09	0.51
	phonon	-0.36	-0.28	-0.71	-0.71	0.97
CdSiN ₂	total	0.39	-0.26	0.07	-0.49	-0.37
	electronic	0.52	-0.07	0.51	-0.07	-0.80
	phonon	-0.13	-0.19	-0.44	-0.42	0.43
CdGeN ₂	total	0.14	-0.16	-0.13	-0.45	0.03
	electronic	0.38	-0.03	0.38	-0.03	-0.46
	phonon	-0.24	-0.13	-0.51	-0.42	0.49
CdSnN ₂	total	-1.11	-1.03	-1.60	-1.51	2.13
	electronic	-0.64	-0.74	-0.63	-0.76	1.32
	phonon	-0.47	-0.29	-0.97	-0.75	0.81

those by Prussel and Véniard [60] for the electronic part only. Their value of $\chi_{zzz}^{(2)}(-\omega, \omega, 0)$ obtained by means of a frequency dependent sum-over-states method neglecting local field effects but including a scissor correction is 9.0 pm/V. Converting this to r_{33} by dividing by $(\epsilon^\infty)^2$ and multiplying by -2 gives -0.68 in agreement with ours even though the method used is rather different.

Next, in Table V, we show the clamped EO coefficients for the II-IV-N₂ compounds at LDA relaxed lattice constants. In addition, we show for each coefficient, its decomposition in the electronic and phonon parts. Here, additional components are nonzero because of the lower symmetry. These were obtained with HGH pseudopotentials. These were not revised because the experimental values for the indices of refraction are not currently available. For the Zn-IV-N₂ compounds they were previously reported by Paudel *et al.* [16]. However, as mentioned earlier for the d_{im} coefficients, we found those results to be poorly converged with respect to the \mathbf{k} -point mesh. Focusing, for example, on ZnGeN₂, which is the closest to GaN, we can see that the electronic part is rather similar to that in GaN. This makes sense because they have very similar band structures. However, the phonon part is rather different. The phonon part is related to the Raman tensor as pointed out in Introduction. The phonon spectrum in ZnGeN₂ is rather different from that in GaN because of the much larger

TABLE VI. Clamped (A) and unclamped (B) linear electro-optical coefficients (pm/V) for Cd-IV-N₂ compounds using FHI-pseudopotential.

Components	CdSiN ₂		CdGeN ₂		CdSnN ₂	
	A	B	A	B	A	B
r_{51}	0.47	0.66	0.14	0.32	-1.30	-1.20
r_{42}	-0.21	-0.07	-0.23	-0.09	-1.56	-1.48
r_{13}	0.16	0.40	-0.12	0.12	-1.74	-1.53
r_{23}	-0.45	-0.22	-0.52	-0.29	-2.05	-1.82
r_{33}	-0.56	-0.95	0.04	-0.35	2.88	2.45

number of vibrational modes, which are all Raman active. Thus it is not surprising that the phonon contributions to the EO coefficient are substantially different in ZnGeN₂ and GaN.

Finally, the clamped and unclamped linear optical electro-optical coefficients of the Cd-IV-N₂ compounds are shown in Table VI. The differences between clamped and unclamped values are significant, indicating that the piezoelectric contribution is not negligible. The piezoelectric constants were reported in Ref. [24] and are indeed relatively high.

IV. CONCLUSION

In this paper, we have shown that the $(2n + 1)$ approach based on the Berry-phase calculation of the polarization, as implemented in ABINIT, gives good agreement for the second-order nonlinear optics coefficients in the static limit with the values obtained from a “sum-over-states” approach including local field effects by Chen *et al.* [7] for BN, AlN, and GaN. The results are also in fair agreement with the few experimental values known for AlN and GaN. The approach is here extended toward InN. We found that in order to obtain reasonable values, a gap correction of InN is essential and one cannot totally rely on the scissor correction to achieve this but needs to start from a pseudopotential that already gives a gap. The predicted results on InN remain highly uncertain because of the strong dependence on the pseudopotential. Nonetheless, the results make sense from the point of view of an approximate linear scaling of the d_{im} coefficients with the inverse gap $1/E_g$. The one previously calculated result for InN [53] would also approximately fall on this linear relationship, keeping into account the larger gap used in that work, which was at that time the commonly accepted experimental band gap value of InN, but which has since been revised.

The effects of the scissor correction in both the $(2n + 1)$ and sum-over-states approach are similar but it is not clear whether it improves agreement with experiment because of the remaining uncertainty on the experimental values and the degree of agreement that can presently be obtained.

The same method was then applied to various II-IV-N₂ semiconductors, with the group-II elements being Mg, Zn, or Cd. The trends in this family are far from trivial. In fact, even for AlN and GaN, they are not obvious because of the large discrepancies of the d_{33}/d_{31} from the quasicubic values in AlN. Unfortunately, there are as yet no experimental values to compare with. Interestingly, MgSiN₂, which should most resemble AlN, shares with it that d_{31} , d_{32} , and d_{33} have the

same sign. We also noticed that the previous calculations reported by Paudel *et al.* [16] for the Zn-IV-N₂ compounds were insufficiently converged with respect to **k** points.

In terms of the Pockels coefficients, we find that the agreement with experiment for AlN and GaN is fair, given again rather large experimental uncertainty. We also find that the phonon and electronic contributions are comparable in magnitude but often of opposite sign. The phonon contributions and electronic contributions were analyzed separately. While the electronic contributions in the II-IV-N₂ and corresponding III-N semiconductors are similar, the phonon contributions are rather different. This reflects the similarity in their band structure but large differences in the phonon spectrum. Finally, we note that even the piezoelectric contribution

appearing in the unclamped value is significant for the Cd-IV-N₂ compounds.

The numerical values of the Pockels coefficient as such are rather unremarkable. They are relatively small compared to the ones in, for example, ferroelectric perovskite oxides where the phonon contribution becomes dominant [34,61].

ACKNOWLEDGMENTS

This work was supported by the National Science Foundation, Division of Materials research under Grant No. 1533957. Calculations made use of the High Performance Computing Resource in the Core Facility for Advanced Research Computing at Case Western Reserve University.

-
- [1] D. E. Aspnes, *Phys. Rev. B* **6**, 4648 (1972).
- [2] J. E. Sipe and E. Ghahramani, *Phys. Rev. B* **48**, 11705 (1993).
- [3] C. Aversa and J. E. Sipe, *Phys. Rev. B* **52**, 14636 (1995).
- [4] J. E. Sipe and A. I. Shkrebtii, *Phys. Rev. B* **61**, 5337 (2000).
- [5] Z. H. Levine, *Phys. Rev. B* **42**, 3567 (1990).
- [6] Z. H. Levine and D. C. Allan, *Phys. Rev. B* **44**, 12781 (1991).
- [7] J. Chen, L. Jönsson, J. W. Wilkins, and Z. H. Levine, *Phys. Rev. B* **56**, 1787 (1997).
- [8] A. Taghizadeh, F. Hipolito, and T. G. Pedersen, *Phys. Rev. B* **96**, 195413 (2017).
- [9] A. Taghizadeh and T. G. Pedersen, *Phys. Rev. B* **97**, 205432 (2018).
- [10] X. Gonze, *Phys. Rev. B* **55**, 10337 (1997).
- [11] X. Gonze and C. Lee, *Phys. Rev. B* **55**, 10355 (1997).
- [12] A. Dal Corso and F. Mauri, *Phys. Rev. B* **50**, 5756 (1994).
- [13] A. Dal Corso, F. Mauri, and A. Rubio, *Phys. Rev. B* **53**, 15638 (1996).
- [14] W. R. L. Lambrecht and A. Punya, in *III-Nitride Semiconductors and their Modern Devices*, edited by B. Gill (Oxford University Press, 2013), Chap. 15, pp. 519–585.
- [15] T. R. Paudel and W. R. L. Lambrecht, *Phys. Rev. B* **78**, 115204 (2008).
- [16] T. R. Paudel and W. R. L. Lambrecht, *Phys. Rev. B* **79**, 245205 (2009).
- [17] A. Punya, W. R. L. Lambrecht, and M. van Schilfgaarde *Phys. Rev. B* **84**, 165204 (2011).
- [18] P. C. Quayle, E. W. Blanton, A. Punya, G. T. Junno, K. He, L. Han, H. Zhao, J. Shan, W. R. L. Lambrecht, and K. Kash, *Phys. Rev. B* **91**, 205207 (2015).
- [19] A. Punya and W. R. L. Lambrecht, *Phys. Rev. B* **88**, 075302 (2013).
- [20] D. Skachkov, A. Punya Jaroenjittichai, L.-y. Huang, and W. R. L. Lambrecht, *Phys. Rev. B* **93**, 155202 (2016).
- [21] S. Lyu and W. R. L. Lambrecht, *Phys. Rev. Mater.* **1**, 024606 (2017).
- [22] S. Lyu and W. R. L. Lambrecht, *J. Appl. Phys.* **123**, 205701 (2018).
- [23] A. P. Jaroenjittichai and W. R. L. Lambrecht, *Phys. Rev. B* **94**, 125201 (2016).
- [24] S. Lyu and W. R. L. Lambrecht, *J. Appl. Phys.* **124**, 055705 (2018).
- [25] N. Feldberg, B. Keen, J. D. Aldous, D. Scanlon, P. A. Stampe, R. Kennedy, R. Reeves, T. D. Veal, and S. Durbin, in *Photo-voltaic Specialists Conference (PVSC), 2012 38th IEEE* (2012) pp. 002524–002527.
- [26] L. Lahourcade, N. C. Coronel, K. T. Delaney, S. K. Shukla, N. A. Spaldin, and H. A. Atwater, *Adv. Mater.* **25**, 2562 (2013).
- [27] P. C. Quayle, K. He, J. Shan, and K. Kash, *MRS Commun.* **3**, 135 (2013).
- [28] A. N. Fioretti, A. Zakutayev, H. Moutinho, C. Melamed, J. D. Perkins, A. G. Norman, M. Al-Jassim, E. S. Toberer, and A. C. Tamboli, *J. Mater. Chem. C* **3**, 11017 (2015).
- [29] S. Lany, A. N. Fioretti, P. P. Zawadzki, L. T. Schelhas, E. S. Toberer, A. Zakutayev, and A. C. Tamboli, *Phys. Rev. Materials* **1**, 035401 (2017).
- [30] R. Qin, H. Cao, L. Liang, Y. Xie, F. Zhuge, H. Zhang, J. Gao, K. Javaid, C. Liu, and W. Sun, *Appl. Phys. Lett.* **108**, 142104 (2016).
- [31] N. Senabulya, N. Feldberg, R. A. Makin, Y. Yang, G. Shi, C. M. Jones, E. Kioupakis, J. Mathis, R. Clarke, and S. M. Durbin, *AIP Adv.* **6**, 075019 (2016).
- [32] S. Chen, P. Narang, H. A. Atwater, and L.-W. Wang *Adv. Mater.* **26**, 311 (2014).
- [33] A. D. Martinez, A. N. Fioretti, E. S. Toberer, and A. C. Tamboli, *J. Mater. Chem. A* **5**, 11418 (2017).
- [34] M. Veithen, X. Gonze, and P. Ghosez, *Phys. Rev. B* **71**, 125107 (2005).
- [35] D. R. Hamann, X. Wu, K. M. Rabe, and D. Vanderbilt *Phys. Rev. B* **71**, 035117 (2005).
- [36] X. Wu, D. Vanderbilt, and D. R. Hamann, *Phys. Rev. B* **72**, 035105 (2005).
- [37] P. Hohenberg and W. Kohn, *Phys. Rev.* **136**, B864 (1964).
- [38] W. Kohn and L. J. Sham, *Phys. Rev.* **140**, A1133 (1965).
- [39] X. Gonze, J. M. Beuken, R. Caracas, F. Detraux, M. Fuchs, G. M. Rignanese, L. Sindic, M. Verstraete, G. Zerah, and F. Jollet, *Comput. Mater. Sci.* **25**, 478 (2002).
- [40] M. Fuchs and M. Scheffler, *Comput. Phys. Commun.* **119**, 67 (1999).
- [41] C. Hartwigsen, S. Goedecker, and J. Hutter, *Phys. Rev. B* **58**, 3641 (1998).
- [42] Y. Fujii, S. Yoshida, S. Misawa, S. Maekawa, and T. Sakudo, *Appl. Phys. Lett.* **31**, 815 (1977).
- [43] J. Miragliotta, D. K. Wickenden, T. J. Kistenmacher, and W. A. Bryden, *J. Opt. Soc. Am. B* **10**, 1447 (1993).
- [44] J. Li, K. B. Nam, M. L. Nakarmi, J. Y. Lin, H. X. Jiang, P. Carrier, and S.-H. Wei, *Appl. Phys. Lett.* **83**, 5163 (2003).

- [45] I. Vurgaftman and J. R. Meyer, *J. Appl. Phys.* **94**, 3675 (2003).
- [46] K. M. Yu, Z. Liliental-Weber, W. Walukiewicz, W. Shan, J. W. Ager, S. X. Li, R. E. Jones, E. E. Haller, H. Lu, and W. J. Schaff, *Appl. Phys. Lett.* **86**, 071910 (2005).
- [47] W. J. Moore, J. A. Freitas, R. T. Holm, O. Kovalenkov, and V. Dmitriev, *Appl. Phys. Lett.* **86**, 141912 (2005).
- [48] A. S. Barker and M. Ilegems, *Phys. Rev. B* **7**, 743 (1973).
- [49] T. L. Tansley and R. J. Egan, *Phys. Rev. B* **45**, 10942 (1992).
- [50] T. Inushima, T. Shiraishi, and V. Davydov, *Solid State Commun.* **110**, 491 (1999).
- [51] S. N. Rashkeev, W. R. L. Lambrecht, and B. Segall, *Phys. Rev. B* **57**, 3905 (1998).
- [52] J. L. P. Hughes and J. E. Sipe, *Phys. Rev. B* **53**, 10751 (1996).
- [53] V. I. Gavrilenko and R. Q. Wu, *Phys. Rev. B* **61**, 2632 (2000).
- [54] S. N. Rashkeev, S. Limpijumnong, and W. R. L. Lambrecht, *Phys. Rev. B* **59**, 2737 (1999).
- [55] E. Dogheche, D. Rémiens, A. Boudrioua, and J. C. Loulergue, *Appl. Phys. Lett.* **74**, 1209 (1999).
- [56] P. Gräupner, J. C. Pommier, A. Cachard, and J. L. Coutaz, *J. Appl. Phys.* **71**, 4136 (1992).
- [57] G. Irmer, C. Röder, C. Himcinschi, and J. Kortus, *Phys. Rev. B* **94**, 195201 (2016).
- [58] X.-C. Long, R. A. Myers, S. R. J. Brueck, R. Ramer, K. Zheng, and S. D. Hersee, *Appl. Phys. Lett.* **67**, 1349 (1995).
- [59] M. Cuniot-Ponsard, I. Saraswati, S.-M. Ko, M. Halbwax, Y. H. Cho, and E. Dogheche, *Appl. Phys. Lett.* **104**, 101908 (2014).
- [60] L. Prussel and V. Vénard, *Phys. Rev. B* **97**, 205201 (2018).
- [61] K. D. Fredrickson, V. V. Vogler-Neuling, K. J. Kormondy, D. Caimi, F. Eltes, M. Sousa, J. Fompeyrine, S. Abel, and A. A. Demkov, *Phys. Rev. B* **98**, 075136 (2018).